Cross-checking the symmetry energy at high densities

Gao-Chan Yong
Institute of Modern Physics, Chinese Academy of Sciences, Lanzhou 730000, China

By considering both the effects of the nucleon-nucleon short-range correlations and the isospin-dependent in-medium inelastic baryon-baryon scattering cross section in the transport model, two unrelated Au + Au experimental measurements at 400 MeV/nucleon beam energy are simultaneously analyzed, a mildly soft symmetry energy ($L(\rho_0) = 37$ MeV) at supra-saturation densities is obtained. This result is compatible with the recent result in Phys. Rev. C **92**, 064304 (2015) by comparing the available data on the electric dipole polarizability with the theoretical predictions.

PACS numbers: 25.70.-z, 21.65.Cd, 21.65.Mn, 21.65.Ef

I. INTRODUCTION

The nuclear symmetry energy describes the single nucleonic energy of nuclei or nuclear matter changes as one replaces protons in a system with neutrons. Besides its impacts in nuclear physics [1, 2], in a density range of 0.1 $\sim$ 10 times nuclear saturation density, the symmetry energy determines the birth of neutron stars and supernova neutrinos [3], a range of neutron star properties such as cooling rates, the thickness of the crust, the mass-radius relationship, and the moment of inertia [4–7]. The nuclear symmetry energy also plays crucial role in the evolution of core-collapse supernova [8] and astrophysical r-process nucleosynthesis [9]. Thus the better we can constrain the symmetry energy in laboratory measurements, the more we can learn from astro-observations.

To constrain the symmetry energy in broad density regions, besides the studies in astrophysics [10–12], many terrestrial experiments are being carried out or planned using a wide variety of advanced new facilities, such as the Facility for Rare Isotope Beams (FRIB) in the US [13], or the Radioactive Isotope Beam Facility (RIBF) in Japan [14]. To unscramble symmetry energy related experimental data, various isospin-dependent transport models are frequently used to probe the symmetry energy below and above saturation density [1, 2]. With great efforts, the nuclear symmetry energy and its slope around saturation density of nuclear matter from 28 analysis of terrestrial nuclear laboratory experiments and astrophysical observations have been roughly pinned down [15], while recent interpretations of the FOPI and FOPI-LAND experimental measurements by different groups made the symmetry energy at supra-saturation densities fall into chaos [16–22]. It does not seem to be clarified why the nuclear symmetry energy at supra-saturation densities is so uncertain, maybe the effects of pion in-medium effects [23–25], the isospin dependence of in-medium nuclear strong interactions [26], the short-range tensor force [27, 28] are some factors.

Recently, the high-momentum transfer measurements showed that nucleons in nucleus can form pairs with large relative momenta and small center-of-mass momenta [29, 30]. This phenomenon was explained by the short-range nucleon-nucleon tensor interaction [31, 32]. Such nucleon-nucleon short-range correlations (SRC) in nucleus lead to a high-momentum tail (HMT) in the single-nucleon momentum distribution [33–36]. More interestingly, in the HMT of nucleon momentum distribution, nucleon component is evidently isospin-dependent. The number of n-p SRC pairs is about 18 times that of the p-p and n-n SRC pairs [37]. And in neutron-rich nucleus, proton has a greater probability than neutron to have momentum greater than the nuclear Fermi momentum [38].

Unfortunately, effects of the above isospin-dependent SRC were seldom taken into account in most of currently used isospin-dependent transport models, while the latters have been frequently used to unscramble symmetry energy related experimental data [17, 20, 39–42]. To extract information on the symmetry energy from experimental data, in this study, by considering both the effects of the isospin-dependent SRC and the important but often-overlooked in-medium baryon-baryon inelastic cross section in the isospin-dependent transport model, two unrelated experimental measurements are simultaneously re-analyzed.

II. THE IBUU TRANSPORT MODEL

To probe the symmetry energy from experimental data, we use our recent updated Isospin-dependent Boltzmann-Uehling-Uhlenbeck (IBUU) transport model [43]. In this IBUU model, nucleon-density distribution is given by

$$r = R(x_1)^{1/3}; cos\theta = 1 - 2x_2; \phi = 2\pi x_3;$$

$$x = rsin\theta cos\phi; y = rsin\theta sin\phi; z = rcos\theta. \qquad (1)$$

Where R is the radius of nucleus, x_1, x_2, x_3 are three independent random numbers. Since there is a depletion of nucleon distribution inside the Fermi sea, the proton and neutron momentum distributions with high-momentum tail reaching about 2 times the Fermi momentum [43] are given by the extended Brueckner-Hartree-Fock (BHF) approach by adopting the AV 18 two-body interaction plus a microscopic Three-Body-Force (TBF) [36]. Fig. 1

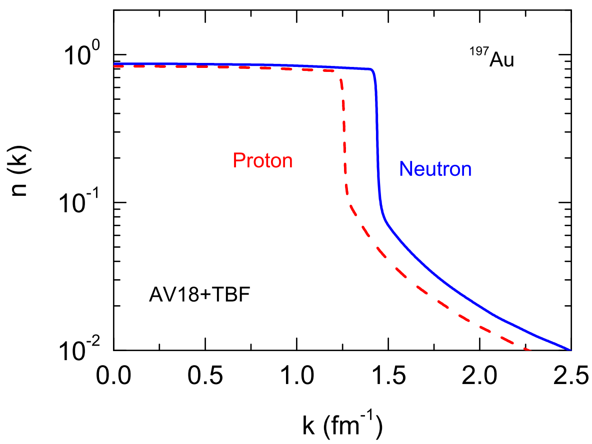

FIG. 1: (Color online) Momentum distributions of neutron and proton in nucleus ^{197}Au calculated with the BHF with Av18+TBF. Taken from Ref. [43].

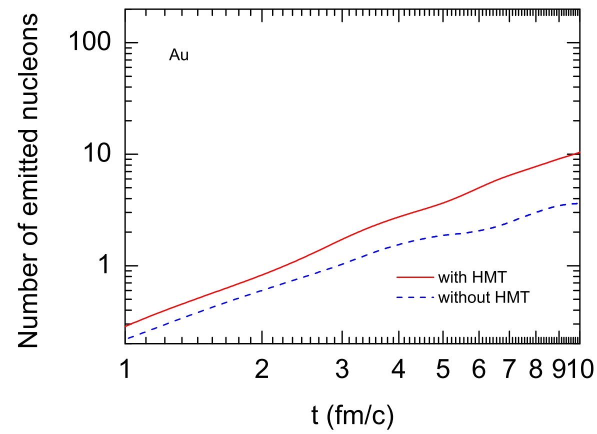

FIG. 3: (Color online) Time dependence of the number of evaporated nucleons by the nucleus in ground state using two initial distributions with and without high momentum tail as shown in Fig. 2.

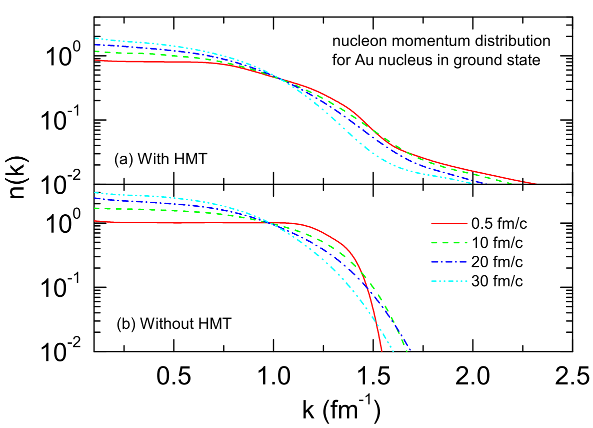

FIG. 2: (Color online) Evolution of the momentum distribution of nucleon in nucleus ^{197}Au. The upper panel (a) is for the case of initial nucleon distribution with HMT while the lower panel (b) is a simple Fermi-Dirac initial distribution. Both cases are under the interaction given by Eq. (2).

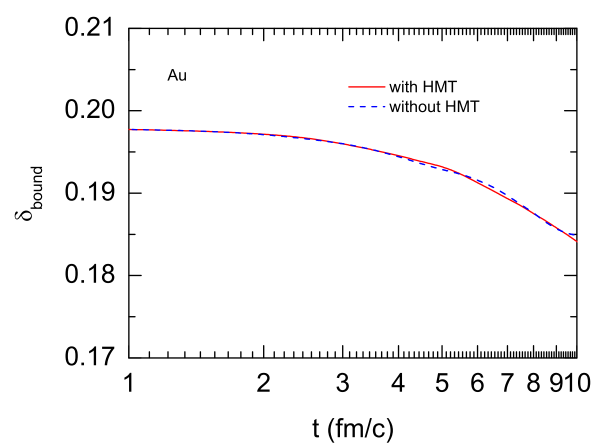

FIG. 4: (Color online) Time dependence of the asymmetry $\delta_{bound} = (\rho_n - \rho_p)/(\rho_n + \rho_p)$ of bound nucleons in the nucleus in ground state using two initial distributions with and without high momentum tail as shown in Fig. 2 and Fig. 3.

shows such nucleon momentum distribution with high-momentum tail in ^{197}Au. Compared with the distribution in ideal Fermi gas, the excess energy of nucleon in colliding nuclei is subtracted from the total energy of reaction system.

How long will survive the shape of the initial distributions? To answer this question, Fig. 2 shows the plots of the implemented distributions at several times (0.5 fm/c, 10 fm/c, 20 fm/c, 30 fm/c) for nuclei in the ground states when they are left to evolve under the interaction given by Eq. (2) in this text and initialized in agreement with the distribution seen in Fig. 1. The lower panel (b) shown in Fig. 2 is under the simple Fermi-Dirac distribution as comparison. It is seen that the shape of the initial distribution of nucleon in momentum space is relatively well kept at the initial stage of collision at 400 MeV/nucleon incident beam energy. Related to the previous point, it is important to show a comparative study of the time dependence of the number of evaporated nucleons by the nuclei in ground state, both when are considered a simple Fermi-Dirac distribution and a distribution with high momentum tail. Shown in Fig. 3 is the

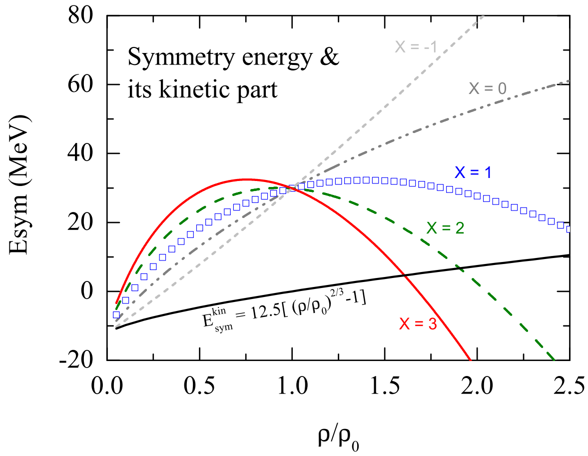

FIG. 5: (Color online) Kinetic symmetry energy and density-dependent symmetry energy with different x parameters. Note here that in heavy-ion collisions at 400 MeV/nucleon beam energy, the high-density part of the symmetry energy plays major role.

time dependence of the number of evaporated nucleons by the nucleus in ground state using two initial distributions with and without high momentum tail. One can clearly see that compared with the case without HMT, more nucleons emit from nucleus with HMT at the initial stage of collision at 400 MeV/nucleon incident beam energy. However, to study the effect of the symmetry energy, the asymmetry ($\delta_{bound} = (\rho_n - \rho_p)/(\rho_n + \rho_p)$) of the colliding system is more crucial. Shown in Fig. 4 is the time dependence of the asymmetry of bound nucleons in the nucleus in ground state using two initial distributions with and without high momentum tail as shown in Fig. 2 and Fig. 3. It is seen that with HMT the asymmetry of colliding nucleons in the reaction system is almost the same as that without HMT at the the initial stage of collision. One can thus conclude that although the present HMT considerations in initial colliding nuclei cause the instability of nuclei, it in fact does not affect much the present study of the symmetry energy at high densities using heavy-ion collisions.

In this model, the isospin- and momentum-dependent mean-field single nucleon potential is used [43–45], i.e.,

$$\begin{aligned} U(\rho,\delta,\vec{p},\tau) &= A_u(x)\frac{\rho_{\tau'}}{\rho_0} + A_l(x)\frac{\rho_\tau}{\rho_0} \\ &+ B(\frac{\rho}{\rho_0})^\sigma(1-x\delta^2) - 8x\tau\frac{B}{\sigma+1}\frac{\rho^{\sigma-1}}{\rho_0^\sigma}\delta\rho_{\tau'} \\ &+ \frac{2C_{\tau,\tau}}{\rho_0}\int d^3\vec{p'}\frac{f_\tau(\vec{r},\vec{p'})}{1+(\vec{p}-\vec{p'})^2/\Lambda^2} \\ &+ \frac{2C_{\tau,\tau'}}{\rho_0}\int d^3\vec{p'}\frac{f_{\tau'}(\vec{r},\vec{p'})}{1+(\vec{p}-\vec{p'})^2/\Lambda^2}, \end{aligned} \quad (2)$$

where $\tau,\tau' = 1/2(-1/2)$ for neutrons (protons), $\delta = (\rho_n-\rho_p)/(\rho_n+\rho_p)$ is the isospin asymmetry, and ρ_n, ρ_p denote neutron and proton densities, respectively. Specifically, the parameter values $A_u(x)$ = 33.037 - 125.34x MeV, $A_l(x)$ = -166.963 + 125.34x MeV, B = 141.96 MeV, $C_{\tau,\tau}$ = 18.177 MeV, $C_{\tau,\tau'}$ = -178.365 MeV σ = 1.265, and Λ = 630.24 MeV/c are obtained by fitting seven empirical constraints of the saturation density $\rho_0 = 0.16$ fm^{-3}, the binding energy E_0 = -16 MeV, the incompressibility K_0 = 230 MeV, the isoscalar effective mass $m_s^* = 0.7m$, the single-particle potential U^0_∞ = 75 MeV at infinitely large nucleon momentum at saturation density in symmetric nuclear matter, the symmetry energy $S(\rho) = 30$ MeV and the symmetry potential U^{sym}_∞ = -100 MeV at infinitely large nucleon momentum at saturation density. $f_\tau(\vec{r},\vec{p})$ is the phase-space distribution function at coordinate $\vec{r}$ and momentum $\vec{p}$ and solved by using the test-particle method numerically [43]. Different symmetry energy's stiffness parameter x can be used in the above single nucleon potential to mimic different forms of the symmetry energy. Since the kinetic symmetry energy, even its sign, is still controversial [46], we at present give it a null value [47]. For its density-dependence, we use similar form as that from the ideal Fermi gas model. Thus the density-dependent kinetic symmetry energy is expressed as

$$E^{kin}_{sym} = 12.5[(\rho/\rho_0)^{2/3} - 1]. \quad (3)$$

Fig. 5 shows the kinetic symmetry energy we used and the density-dependent symmetry energy with different x parameters. It is seen that our used density-dependent kinetic symmetry energy is similar to that in Ref. [46, 48]. We can also see that $x = 1, 0, -1$ cases roughly correspond positive slopes ($L(\rho_0) \equiv 3\rho_0 dEsym(\rho)/d\rho$) 37, 87, 138 MeV, respectively. The following table shows the parameters used in Eq. (2) with SRC compared with the case without SRC [44].

TABLE I: The parameters (in MeV) used in Eq. (2) with SRC compared with the case without SRC [44].

E^{kin}_{sym}	0 (= with SRC)	12.5 $(\rho/\rho_0)^{2/3}$ (= without SRC)
$A_u(x)$	33.037 - 125.34x	-95.98 - 91.157x
$A_l(x)$	-166.963 + 125.34x	-120.57 + 91.157x
B	141.96	106.35
$C_{\tau,\tau}$	18.177	-11.7
$C_{\tau,\tau'}$	-178.365	-103.4
σ	1.265	1.333
Λ	630.24	260

The isospin-dependent baryon-baryon (BB) scattering cross section (elastic or inelastic, including NN→NN, NΔ→NΔ, ΔΔ→ΔΔ, NN⇌NΔ) in medium σ^{medium}_{BB} is reduced compared with their free-space value σ^{free}_{BB} by a factor of [43]

$$\begin{aligned} R^{BB}_{medium}(\rho,\delta,\vec{p}) &\equiv \sigma^{medium}_{BB_{elastic,inelastic}}/\sigma^{free}_{BB_{elastic,inelastic}} \\ &= (\mu^*_{BB}/\mu_{BB})^2, \end{aligned} \quad (4)$$

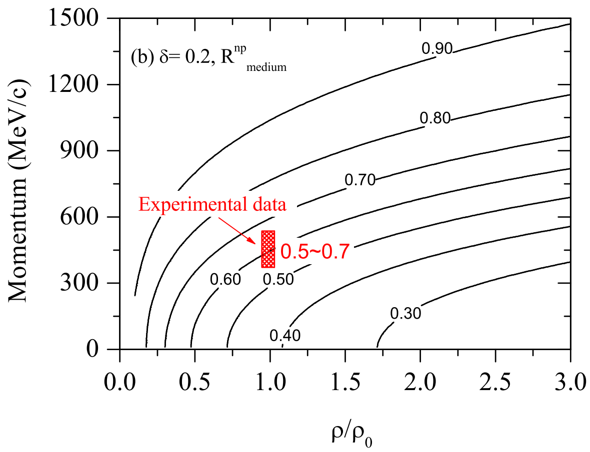

FIG. 6: (Color online) Reduced factor R^{np}_{medium} of neutron-proton scattering cross section as a function of density and nucleonic momentum in asymmetric medium $\delta = 0.2$. The red shadow region and label '0.5∼0.7' denote experimental density and momentum region and the corresponding value of reduced factor R^{np}_{medium}.

where μ_{BB} and μ^{*}_{BB} are the reduced masses of the colliding baryon-pair in free space and medium (in medium, the effective mass of baryon is used), respectively. The effective mass of baryon in isospin asymmetric nuclear matter is expressed by

$$\frac{m^{*}_{B}}{m_B} = \left\{1 + \frac{m_B}{p}\frac{dU_B}{dp}\right\}. \tag{5}$$

For the baryon resonance Δ potential, the forms of

$$U_B^{\Delta^-} = U_n, \tag{6}$$
$$U_B^{\Delta^0} = \frac{2}{3}U_n + \frac{1}{3}U_p, \tag{7}$$
$$U_B^{\Delta^+} = \frac{1}{3}U_n + \frac{2}{3}U_p, \tag{8}$$
$$U_B^{\Delta^{++}} = U_p \tag{9}$$

are used [49]. As an example, the reduced factor $R^{np}_{medium}(\rho, \delta, \vec{p})$ of neutron-proton scattering cross section in medium is shown in Fig. 6. It is a function of density and nucleonic momentum in medium with asymmetry $\delta = 0.2$ for example. And generally $R^{nn}_{medium} > R^{np}_{medium} > R^{pp}_{medium}$ at certain density and momentum. The nucleon-nucleon scattering cross section is reduced much in medium for colliding pair at high density and low momentum while it is less reduced at low density and high momentum. It is noticed from Fig. 6 that the used in-medium neutron-proton scattering cross section fits the experimental hard photon measurements quite well [50].

III. RESULTS AND DISCUSSIONS

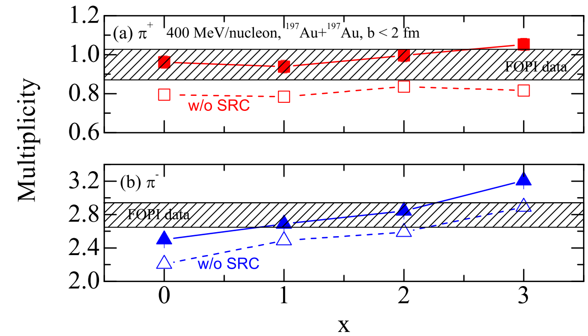

FIG. 7: (Color online) Multiplicity of charged pion meson produced in Au+Au reaction at 400 MeV/nucleon with different symmetry energies. The shadow region denotes the FOPI data [51]. The dashed lines show the cases without SRC.

Before studying the π^-/π^+ ratio, it is instructive to first see the production of charged pion meson in central Au + Au reaction at 400 MeV/nucleon beam energy. Fig. 7 shows numbers of charged pion produced with different symmetry energies. It is seen that for x = 1 and x = 2 cases both produced π^- and π^+ fit the FOPI experimental data quite well. With stiffer symmetry energy $x = 0$, the model gives somewhat smaller π^- number than experimental data. While with very soft symmetry energy $x = 3$, the model gives both larger π^+ and π^- numbers than experimental data. Comparing upper panel with lower panel, it is seen that sensitivity of the number of produced π^- to the symmetry energy is at least 3 times that of π^+. This is because the π^- mesons are mostly produced from neutron-neutron collisions, thus more sensitive to the isospin asymmetry of the reaction system and the symmetry energy [52]. From this figure, one can see that without SRC, numbers of both π^+ and π^- are smaller than those with SRC. This is understandable since the SRC of nucleons increases the kinetic energy of nucleon.

To reduce the systematic errors, most of the observables proposed so far use differences or ratios of isospin multiplets of baryons, mirror nuclei and mesons, such as, the neutron/proton ratio of nucleon emissions, neutron-proton differential flow, π^-/π^+, etc. Fig. 8 shows the π^-/π^+ ratio predicted by our IBUU model with different symmetry energies. Because softer symmetry energy causes more neutron-rich dense matter and π^-'s are mainly from neutron-neutron collision whereas π^+'s are mainly from proton-proton collision [52], it is not surprising that one sees larger π^-/π^+ ratio with softer symmetry energy. To see the effects of SRC of nucleon-nucleon and the reduction of the in-medium inelastic baryon-baryon scattering cross section, with same x parame-

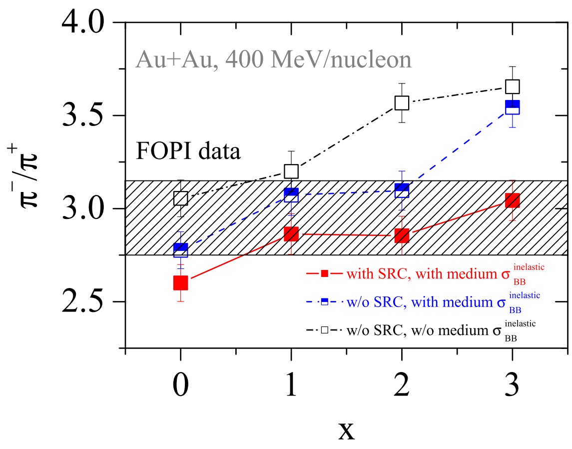

FIG. 8: (Color online) π^-/π^+ ratio in Au+Au reaction at 400 MeV/nucleon with different symmetry energies. Also shown are the effects of the SRC of nucleon-nucleon and the in-medium inelastic cross section on the π^-/π^+ ratio with same x parameters.

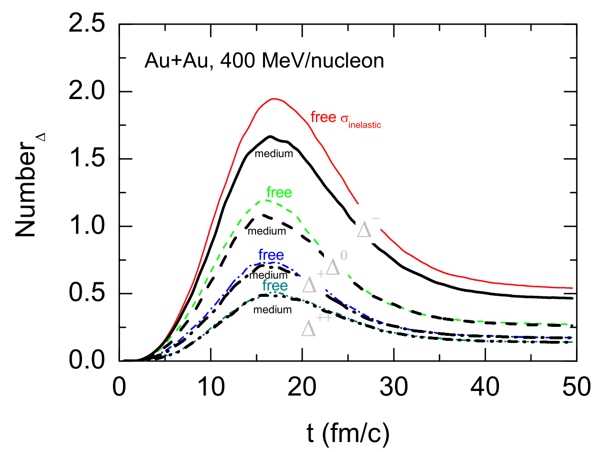

FIG. 9: (Color online) The effects of in-medium inelastic cross section on the productions of different Δ resonance in Au+Au reaction at 400 MeV/nucleon with the symmetry energy parameter $x = 1$.

ters, we made calculations by turning off the SRC and the reduction of the in-medium inelastic baryon-baryon scattering cross section, respectively. From Fig. 8, we can see that both of them affect the value of π^-/π^+ ratio evidently. Both the SRC of nucleon-nucleon and the reduction of the in-medium inelastic baryon-baryon scattering cross section decrease the value of π^-/π^+ ratio evidently. Proton-proton collision is also affected by the Coulomb action, so π^+ production, which is mainly from proton-proton collision, is relatively less affected by the reduction of the in-medium inelastic baryon-baryon scattering cross section. Fig. 9 shows the evolution of Δ resonance production with free and in-medium inelastic cross sections. It is clear seen that the in-medium inelastic cross section affects the production of Δ^- (decay into π^-) much than Δ^{++} (decay into π^+). This is the reason why the reduced in-medium inelastic baryon-baryon cross section decreases the value of π^-/π^+ ratio. The SRC of neutron and proton causes small asymmetry of matter, which corresponds small value of π^-/π^+ ratio. Therefore both the SRC of nucleon-nucleon and the in-medium inelastic baryon-baryon cross sextion should be taken into account in transport calculations. From Fig. 8, we can see that the FOPI pion experimental data supports a softer symmetry energy ($x = 1$, 2, even $x = 3$). Note here that the density region probed here is about $1 \sim 1.5$ times saturation density [53]. So we do not conclude what are the constraints of the values of the symmetry energy and its slope around saturation density.

While $\triangle$ and π's scattering and re-absorption can destroy the high density signal in a certain degree. Treatment of Delta dynamics in transport models is not so straightforward such as the competing effects of the mean fields and $\triangle$ thresholds. To understand quantitatively the symmetry energy effect on pion production, it is important to include the isospin-dependent pion in-medium effects [23–25]. And recent work of MSU group [54] demonstrates that the ratio of π's spectra is more sensitive than the ratio of integrated yields because the latter gives ambiguous result since it does not distinguish π's messenger of high density from the rest. Therefore, more theoretical and experimental studies are needed to pin down the high-density behavior of the symmetry energy by pion probe.

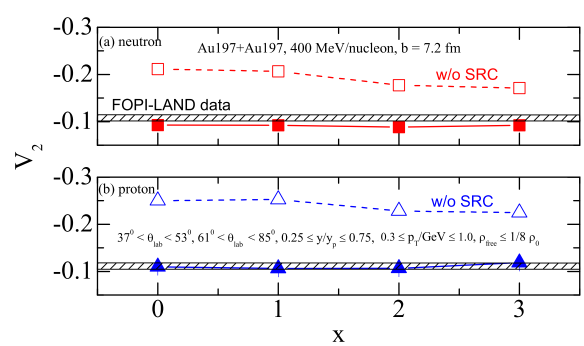

FIG. 10: (Color online) Elliptic flow of emitting nucleons in Au+Au collision at 400 MeV per nucleon incident beam energy with different symmetry energies. The shadow region denotes the experimental FOPI-LAND data [20]. The dashed lines show the cases without SRC.

To cross-check the symmetry energy over a broad region ($x = 1$, 2, 3), one has to search for other constraints.

Fig. 10 shows predicted neutron and proton elliptic flows in Au + Au reaction under the FOPI-LAND experimental conditions (here we use the data with b = 7.2 fm case) and geometry [20]. The experimental data was multiplied by a factor 1.15 owing to dispersion of the reaction plane [55]. From Fig. 10 (a), it is seen that our model give somewhat lower value of the elliptic flow of neutrons. However, from Fig. 10 (b), it is seen that the predicted elliptic flow of protons fit experimental data quite well. In our model, free nucleons are identified by their local densities $\rho_{free} \leq \rho_0/8$, which corresponding to deuteron's nucleon average density $0.02 fm^{-3}$. The identification standard of free nucleons affects the value of V_2^n and V_2^p, but does not affect the ratio of V_2^n/V_2^p much. With stiffer symmetry energy, the value of nucleon elliptic flow should become larger. However, this trend seems not right for the stiffer symmetry energy $x = 0$. This abnormal behavior may be caused by the competing effects of the SRC and the symmetry energy and deserve further study. From Fig. 10, at such experimental conditions and geometry, effects of the symmetry energy on both proton and neutron elliptic flows can not be seen clearly. One way to enlarge the effects of the symmetry energy is the relative changes of proton and neutron elliptic flows, such as the ratio of neutron and proton elliptic flows V_2^n/V_2^p. From this figure, one can see that without SRC, values of both neutron elliptic flow and proton elliptic flow are larger than those with SRC. This is understandable since the SRC of nucleons decreases the anisotropic emissions of neutrons and protons.

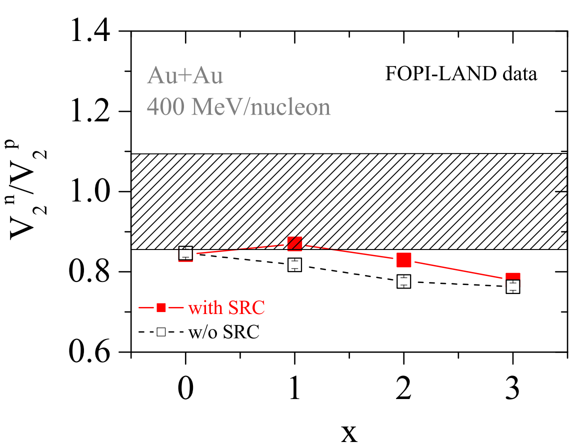

FIG. 11: (Color online) Same as Fig. 10, but for the ratio of V_2^n/V_2^p. The effects of the SRC of nucleon-nucleon on the V_2^n/V_2^p with same x parameters are also shown.

Shown in Fig. 11 is predicted elliptic flow ratios of neutron and proton V_2^n/V_2^p with different symmetry energies as well as experimental data [20]. Since stiffer symmetry energy/symmetry potential causes relatively more neutrons to emit in the direction perpendicular to the reaction plane [56], one sees larger values of elliptic flow ratios of neutron and proton V_2^n/V_2^p with stiffer symmetry energies. With the SRC of nucleon-nucleon in the transport model, values of the V_2^n/V_2^p ratio are larger than that without the SRC of nucleon-nucleon. This is because the SRC of nucleon-nucleon cause neutron and proton to be correlated together, the value of V_2^n/V_2^p ratio trends to unity. Owing to the competing effects of the SRC and the symmetry energy, for $x = 0$ case, the effects of symmetry energy on the trend of the ratio of V_2^n/V_2^p with the SRC changes compared with that without the SRC.

On the whole, the sensitivity of the observable V_2^n/V_2^p to the symmetry enegy at FOPI-LAND experimental conditions and geometry is smaller than that of the FOPI π^-/π^+ ratio. Other nucleon observables should be further explored.

Fig. 11 indicates the FOPI-LAND elliptic flow experimental data does not favor very soft symmetry energy (x = 2, 3). Combining the studies of nucleon elliptic flow and previous π^-/π^+ ratio, one may roughly obtain the symmetry energy stiffness parameter $x = 1$. It in fact corresponds a mildly soft density-dependent symmetry energy at supra-saturation densities. While the specific density region of the present constraints on the nuclear symmetry energy needs to be further studied [53].

The small effects of the symmetry energy on pionic and nucleonic observables, pion suffering from unclear $\pi - N - \Delta$ dynamics and pion in-medium effect, neutron detection efficiency, bound or unbound nucleon identifications, nucleon in-medium and isospin strong interactions as well as all kinds of experimental measurement errors, etc., all affect the probe of the symmetry energy, not to mention uncertainties and complexities of nuclear transport models, thus fully convincing constraints of the symmetry energy at high-density are not easy to achieve.

It is, however, interesting to see that the present result on the symmetry energy stiffness parameter $x = 1$ (which corresponds a slope of symmetry energy at saturation density ($L(\rho_0) \equiv 3\rho_0 dEsym(\rho)/d\rho = 37$ MeV) agrees with the recent result $L(\rho_0) = 20 - 66$ MeV quite well by comparing the available data on the electric dipole polarizability with the predictions of the random-phase approximation, using a representative set of nuclear energy density functionals [57].

IV. CONCLUSIONS

In summary, by incorporating the short-range correlations of nucleon-nucleon and the in-medium inelastic baryon-baryon scattering cross section into the isospin-dependent transport model and based on the FOPI and FOPI-LAND experimental measurements, I cross-checked the π^-/π^+ ratio and the ratio of neutron elliptic flow and proton elliptic flow V_2^n/V_2^p in Au+Au collision. A mildly soft symmetry energy at supra-saturation densities supports both FOPI and FOPI-LAND experi-

mental measurements. The studies also show that both the short-range correlations of nucleon-nucleon and the in-medium inelastic baryon-baryon cross section play important role in probing the symmetry energy with heavy-ion collisions.

Since the symmetry energy plays crucial roles in both nuclear physics and astrophysics, more subjects, such as the density region that some observables probed and more sensitive observables to the symmetry energy at high densities, deserve further study.

Acknowledgements

The author thanks M. D. Cozma for providing the FOPI-LAND elliptic flow analysis routine and helpful discussions. The work was carried out at National Supercomputer Center in Tianjin, and the calculations were performed on TianHe-1A. The work is supported by the National Natural Science Foundation of China under Grant Nos. 11375239, 11435014.

[1] V. Baran, M. Colonna, V. Greco, M. Di Toro, Phys. Rep. **410**, 335 (2005).
[2] B. A. Li, L. W. Chen and C. M. Ko, Phys. Rep. **464**, 113 (2008).
[3] K. Sumiyoshi, H. Suzuki, H. Toki, Astron. Astrophys. **303**, 475 (1995).
[4] K. Sumiyoshi and H. Toki, Astrophys. J. **422**, 700 (1994).
[5] J. M. Lattimer, M. Prakash, Science **304**, 536 (2004).
[6] A. W. Steiner, M. Prakash, J. M. Lattimer, P. J. Ellis, Phys. Rep. **411**, 325 (2005).
[7] James M. Lattimer, Andrew W. Steiner, Eur. Phys. J. A **50**, 40 (2014).
[8] T. Fischer et al., Eur. Phys. J. A **50**, 46 (2014).
[9] N. Nikolov, N. Schunck, W. Nazarewicz, M. Bender, and J. Pei, Phys. Rev. C **83**, 034305 (2011).
[10] Andrew W. Steiner, James M. Lattimer, and Edward F. Brown, ApJ. 722, 33, (2010).
[11] F. J. Fattoyev, J. Carvajal, W. G. Newton, Bao-An Li, Phys. Rev. C **87**, 015806 (2013).
[12] F. J. Fattoyev, W. G. Newton, Bao-An Li, Eur. Phys. J. A, **50**, 45 (2014).
[13] G. Bollen, AIP Conf. Proc. 1224, 432 (2010).
[14] Yasushige Yano, Nuclear Instruments and Methods in Physics Research B 261, 1009 (2007).
[15] B. A. Li, X. Han, Phys. Lett. B **727**, 276 (2013).
[16] W. M. Guo, G. C. Yong, Y. J. Wang, Q. F. Li, H. F. Zhang, W. Zuo, Phys. Lett. B **738**, 397 (2014).
[17] Z. G. Xiao, B. A. Li, L. W. Chen, G. C. Yong, M. Zhang, Phys. Rev. Lett. **102**, 062502 (2009).
[18] Z. Q. Feng, G. M. Jin, Phys. Lett. B 683, 140 (2010).
[19] P. Russotto, P. Z. Wu, M. Zoric, M. Chartier, Y. Leifels, R. C. Lemmon, Q. Li, J. Lukasik, A. Pagano, P. Paw lowski, W. Trautmann, Phys. Lett. B 697, 471 (2011).
[20] M. D. Cozma, Y. Leifels and W. Trautmann, Q. Li, P. Russotto, Phys. Rev. C 88, 044912 (2013).
[21] W. J. Xie, J. Su, L. Zhu, F. S. Zhang, Phys. Lett. B 718, 1510 (2013).
[22] Y. J. Wang, C. C. Guo, Q. F. Li, H. F. Zhang, Y. Leifels, and W. Trautmann, Phys. Rev. C **89**, 044603 (2014).
[23] J. Xu, L. W. Chen, C. M. Ko, B. A. Li, Y. G. Ma , Phys. Rev. C **87**, 067601 (2013).
[24] W. M. Guo, G. C. Yong, and W. Zuo, Phys. Rev. C **91**, 054616 (2015).
[25] Jun Hong, P. Danielewicz, Phys. Rev. C **90**, 024605 (2014).
[26] G. C. Yong, W. Zuo, X. C. Zhang , Phys. Lett. B, **705**, 240 (2011).
[27] V. R. Pandharipande and V. K. Garde, Phys. Lett. B, **39**, 608 (1972).
[28] C. Xu, B. A. Li, `http://arxiv.org/abs/1104.2075`, arXiv:1104.2075 (2011).
[29] E. Piasetzky, M. Sargsian, L. Frankfurt, M. Strikman, J. W. Watson, Phys. Rev. Lett. **97**, 162504 (2006).
[30] R. Shneor et al., Phys. Rev. Lett. **99**, 072501 (2007).
[31] M. M. Sargsian, T. V. Abrahamyan, M. I. Strikman and L. L. Frankfurt, Phys. Rev. C **71**, 044615 (2005).
[32] R. Schiavilla, R. B. Wiringa, S. C. Pieper and J. Carlson, Phys. Rev. Lett. **98**, 132501 (2007).
[33] H. A. Bethe, Ann. Rev. Nucl. Part. Sci. **21**, 93 (1971).
[34] A. N. Antonov, P. E. Hodgson and I. Z. Petkov, *Nucleon Momentum and Density Distributions in Nuclei* (Clarendon Press, Oxford, 1988).
[35] A. Rios, A. Polls, and W. H. Dickhoff, Phys. Rev. C **79**, 064308 (2009).
[36] P. Yin, J. Y. Li, P. Wang, and W. Zuo, Phys. Rev. C **87**, 014314 (2013).
[37] R. Subedi et al. (Hall A. Collaboration), Science **320**, 1476 (2008).
[38] O. Hen et al. (The CLAS Collaboration), Science **346**, 614 (2014).
[39] D. V. Shetty, S. J. Yennello, and G. A. Souliotis, Phys. Rev. C **76**, 024606 (2007).
[40] M. B. Tsang et al., Phys. Rev. Lett. **102**, 122701 (2009).
[41] W. G. Lynch et al., Prog. Part. Nucl. Phys. **62**, 427 (2009).
[42] J. B. Natowitz et al., Phys. Rev. Lett. **104**, 202501 (2010).
[43] G. C. Yong, arXiv: 1503.08523 (2015).
[44] C. B. Das, S. DasGupta, C. Gale, B. A. Li, Phys. Rev. C **67**, 034611 (2003).
[45] J. Xu, L. W. Chen, B. A. Li, Phys. Rev. C **91**, 014611 (2015).
[46] O. Hen, B. A. Li, W. J. Guo, L. B. Weinstein, and E. Piasetzky, Phys. Rev. C 91, 025803 (2015).
[47] I. Vidana, A. Polls, C. Providencia, Phys. Rev. C **84**, 062801 (R) (2011).
[48] A. Carbone, A. Polls, and A. Rios, Europhys. Lett. **97**, 22001 (2012).
[49] W. M. Guo, G. C. Yong, W. Zuo, Phys. Rev. C **92**, 054619 (2015).
[50] G. C. Yong, W. Zuo, X. C. Zhang, Phys. Lett. B **705**, 240 (2011).
[51] W. Reisdorf et al. (FOPI Collaboration), Nucl. Phys. A **848**, 366 (2010).
[52] B. A. Li, G. C. Yong, W. Zuo, Phys. Rev. C **71**, 014608 (2005).
[53] H. L. Liu, G. C. Yong, D. H. Wen, Phys. Rev. C **91**, 044609 (2015).

[54] P. Danielewicz and J. Hong, http://nusym15.ifj.edu.pl/contributions/uploads/PawelDanielewiczNuSYM15.pdf (2015).

[55] M. D. Cozma, private communications

[56] G. C. Yong, B. A. Li, L. W. Chen, Phys. Lett. B **650**, 344 (2007).

[57] X. Roca-Maza, X. Viñas, M. Centelles, B. K. Agrawal, G. Colò, N. Paar, J. Piekarewicz and D. Vretenar, Phys. Rev. C **92**, 064304 (2015).